

Numerical Simulations of Cardiac Dynamics. What Can We Learn from Simple and Complex Models?

F H Fenton

Hofstra University, Hempstead NY, USA

Abstract

Modeling the electrical activity of the heart, and the complex signaling patterns that underlay dangerous arrhythmias such as tachycardia and fibrillation, requires a quantitative model of action potential propagation. At present, there exist detailed ionic models of the Hodgkin-Huxley form that accurately reproduce dynamical features of the action potential at a single cell level. However, such models are very time consuming in computer simulations. We show how simplified models can help on the study of cardiac arrhythmias. In particular, how breakup of spiral waves, believed as the dynamics underlying the transition from tachycardia to fibrillation, can occur as function of tissue size and shape. We also discuss some of the limitations in these models and some differences in dynamics between simple and complex models.

1. Introduction

The study of cardiac arrhythmias using computer models originated in the mid 1940's when Wiener and Rosenblueth [1] used a very simple cellular automata model to describe the propagation of action potentials and investigate under which conditions flutter and fibrillation could arise. Eventhough their model considered homogenous cells with only three dynamical states (excited, refractory and unexcited) and produced a constant conduction velocity as well as a constant duration of action potential. It was enough to explain how electrical waves could re-circulate around obstacles and give a theoretical frame work for the circulating impulses in cardiac tissue observed experimentally by Mines [2] and Garrey [3] in 1914.

Since then, many numerical simulations of cardiac dynamics have helped in many ways to our understanding of arrhythmias. For example in 1964 Moe et al. [4] used a cellular automata similar to [1] but added two more rules, (i) the absolutely-refractory state lasted certain amount of time R which varied randomly from cell to cell, and (ii) four extra intermediate "relatively-refractory" states were considered. This produced a spatially inhomogeneous tissue with dispersion of recovery and variable conduction speed (CV). As the dispersion in values of the refractory times

R increases, Moe's model can produce circulating waves with out the need of any anatomical obstacle (spiral waves), further more at a higher dispersion, breakup of spiral waves occurs leading to a state of multiple wavelets. Moe's model shows how tissue irregularities and variability in CV facilitates the induction of fibrillation. In the late 1960's and 1970's many numerical simulations of continuous generic excitable models showed the existence of spiral waves in isotropic tissue. And in the early 1990's simulations with ionic models showed that steep restitution of action potential duration (APD) (slope > 1) can produce large wave oscillations which can then lead to conduction blocks and spiral wave breakup [5-6] (see Fig.1).

1.1. Ionic Models.

In 1952 Hodgkin and Huxley [7] introduced the first continuous mathematical model designed to reproduce cell membrane action potentials. Since then, there has been many complex models developed for cardiac cells following their approach. Most of these models can be separated into three classes. 1) "First generation" of ionic models, which reproduce basic ionic currents and concentrations like the Beeler-Reuter (BR) [8] and the Luo-Rudy-I (LR-I) [9] models. 2) "Second generation" models, which are more robust since they not only include more currents but also pumps and exchangers for dynamic ionic concentrations like the DiFrancesco-Noble [10]. And 3) simplified models that only use the minimum set of phenomenological currents necessary to reproduce mesoscopic characteristics of cell dynamics such as AP and CV restitutions [11-12].

Simulations using first and second generation models are in general very computationally intensive, specially in 2 and 3 dimensions, therefore it is always desirable to isolate the minimum key features necessary to characterize specific phenomena by using simplified models. Nevertheless it is important to keep in mind that when reducing a complex model some intrinsic behavioral dynamics may be lost. The purpose of this latter is to show some of the advantages and limitations when using simplified models of cardiac action potentials.

2. What can we learn from simplified

models?

The simplified model used in here is a three variable simple ionic model (3V-SIM) developed in [11] which can reproduce arbitrary monophasic APD and CV restitutions by varying some of its parameters. The total membrane current of the model is given by the sum of three phenomenological independent currents: $I_{total} = I_{fi}(U,v)+I_{so}(U)+I_{si}(U,w)$. Where U represents the membrane voltage and, v and w two gate variables. $I_{fi}=-4*p*v*(U-.1)*(1-U)$ corresponds to a fast inward (Na) current, $I_{so}=0.04*(U-0.03272/0.04)*exp(-2U) + 0.03272$, corresponds to a slow outward (K) current, and $I_{si}=-w*(1+tanh(10*(U-0.859)))/44.15$ a slow inward (Ca) current. The gates v and w govern the activation and inactivation of their corresponding currents and their kinetics are given by $\partial_t v = (1-p)*(1-v)/((1-q)*18.5 + q*177)-p*v/3$ and $\partial_t w = (1-p)*(1-w)/37-p*w/645.13$. The membrane voltage follows the cable equation $\partial_t U = \partial_{xj} (D_{ij} \partial_{xj} U) - I_{total} / C_m$. Where D_{ij} is the diffusion tensor, $C_m = 1 \mu F / cm^2$, p and q are Heaviside step functions defined by $p=1$ ($p=0$) for $U \geq Uq$ ($U < Uq$) and $q=1$ ($q=0$) for $U \geq Up$ ($U < Up$), $Uq=0.1$, $Up=0.033$ and U needs to be scale as $U*100-85$ when comparing with ionic models. The model as given above, reproduces the same APD and CV restitution as the eight-variable Beeler-Reuter model[8] (see Fig. 1)

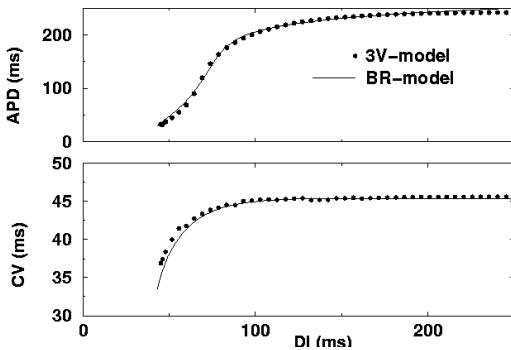


Fig. 1. APD restitution function indicates the duration of an AP as function of the time between activations, known as diastolic interval (DI) and CV restitution indicates the velocity of the wave front as function of the DI. In A) we show the APD restitution and in B) the CV restitution for the 3V-SIM and the BR-model. The curves were obtained by pacing at shorter and shorter DI's as in [11]. Using $D_i = 1 cm^2 / sec$, $dx=0.25$ and $dt= 0.13, 0.75$ for the 3V-SIM and the BR-model respectively.

2.1. One-dimensional rings of cardiac tissue

In 1988 Frame and Simson [13] not only showed, as Mines [2] and Garrey [3], circulating impulses using

rings of canine heart muscle, but also oscillations on the impulse rotation cycle. These oscillations can be explained in terms of the APD and CV restitution [14]. The oscillations are the result of a Hopf bifurcation present when the APD restitution has a slope >1 . Figure 2 shows these oscillations using the BR-model and the 3V-model. We can see that the 3V-model reproduces in a good approximation the amplitude and modulations of the APD oscillations obtained with the BR-model. This oscillations increase as the ring diameter decreases, up to a size of 13.25 cm, where the ring is too small to support a propagating wave. It can be easily shown [5] that by decreasing the steepness of APD restitution, the oscillations can be suppressed. It is important to note that the time needed to simulate 300 rotations using a 600 MHz Alpha is about 6.5 min. for the 3V-model and 54 min. for the BR-model (using $m(t) = m_\infty$, which allows the use of a larger dt [11]), a ratio of about 8.3 times faster using the 3V-model. This ratio becomes very significant when attempting large-scale simulations in three-dimensions.

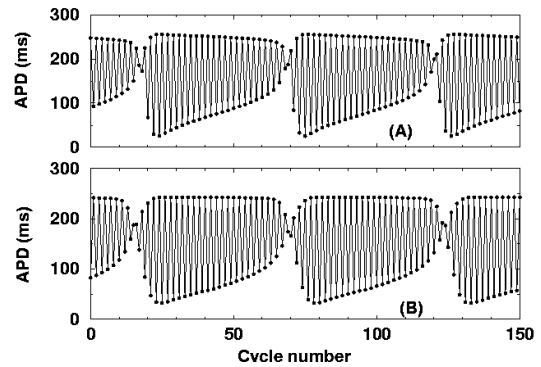


Fig. 2. Oscillations of APD as function of cycle number (one beat to the next) for a simulated ring of cardiac tissue with $L= 12.2$ cm using the BR-model (A) and the 3V-model (B).

2.2. Two-dimensional sheets of cardiac tissue

Simulations of the BR-model in two-dimensional homogeneous sheets of tissue [15] have shown that spiral waves are unstable and readily breakup into multiples because of the AP oscillations produced by the steep APD restitution [5]. The 3V-model also produces unstable spiral waves that break much in the same way. Courtemanche and Winfree [15] showed that when the calcium current in the BR-model is speeded up by two (known as MBR-model), spiral waves become stable. Similarly with the 3V-model, one can vary some of its parameters [11-12] and closely reproduce the restitutions of the MBR-model. In this case the simplified model also leads to stable spiral waves with the same range of frequency rotation, shape and size as the MBR-model [11-12].

Since simulations using the 3V-model are much faster

than with the MBR-model, we used it to study the stability of spiral wave as function of tissue size and periodic boundary conditions by simulating a cylindrical ventricle with out thickness. For cylinders with a perimeter larger than the spiral's wave length, we found no difference in dynamics when compared to a spiral rotating on a square sheet of tissue with zero flux boundary conditions. Nevertheless, when the perimeter is compared to the wavelength, then the spiral wave tip becomes perturbed by the incoming waves generated by itself. The collision of incoming waves, with a higher frequency than the one of rotation, produces a drift on the spiral wave. It has been shown [16] that the drift of a spiral is proportional to the high frequency pacing. Therefore the drift is proportional only to the ratio between the cylinder's perimeter and the length of the wave-tip-trajectory (spiral core) and independent of the shape. Different tip trajectories can be induced in the BR-model as well as in the 3V-model by varying the sodium conductance [11-12]. We have checked that in all cases drift is present when the perimeter is comparable to the core of the spiral.

For cylindrical perimeters smaller than the tip trajectory, it is not possible to maintain a spiral wave, however when a spiral is in the hypermeander regime, there is a window of perimeter sizes between the drift and termination, for which stable-drifting spirals will break. The breakup is produced because the hypermeander wave repolarizes unevenly some regions along the cylinder, therefore incoming waves produced by itself can block the wave tip front and form new spiral waves. This mechanism for breakup can occur in the ventricles when a spiral wave is created close to the apex where the ventricular perimeter decreases. We have checked that the MBR-model also produces the same effect of breakup on a tissue with equal size to the one used with the 3V-model (a perimeter of about 4cm).

2.3. Three-dimensional slabs of cardiac tissue

We have also studied the stability of spiral waves in three-dimensions considering a slab of cardiac tissue and including the natural rotational anisotropy of the fibers [11-12,17]. By using the 3V-model fitted to the MBR-model we found that stable scroll waves (spiral waves in 3D) become unstable and break into multiple as function of tissue thickness and rotation anisotropy. This is in agreement with various experiments of thinning ventricular tissue similar to Garrey's [3] where it is shown that VT degenerates into VF if the tissue is thick however VT remains stable if the tissue is thin.

We found that for thick slabs of tissue with little rotational anisotropy the scroll wave vortex (the equivalent of the spiral wave tip, which becomes a line in 3D) is stable to perturbations and behaves similarly as in a two-dimensional sheet. However, as the rotational

anisotropy is increased, the vortex elongates and curves because of a highly localized twist induced by the fiber rotation. This elongated vortices collide with the tissue boundaries and produce a wave breakup which then leads to multiple waves characteristic of VF. To illustrate the nature of the twist that produces the filament instability we show in Fig. 3a the contour of a spiral wave rotating in the epi-cardium and superimposed the one from the endo-cardium. The spiral wave is from the 3V-model fitted to the MBR-model with sodium conductance changed from 4 to 2.47 (see I_{fi}) [12] so the spiral tip, follows a circular core (in this case distorted ellipses because of the tissue anisotropy with a 1:0.33 ratio). The figure shows how the major axes of the ellipses are rotated by an angle which is roughly equal to the total fiber rotation angle. It also shows how the anisotropic velocity induces a phase difference between the spiral in the epi- and endo-cardium. Therefore when the spiral wave turns around the highly curved part of the distorted ellipse (pivot turn) a twist is produced because the wave front on the epi- leads in time the pivot turn on the endo-cardium. Notice how in the figure the spiral in the epi- already finish the turn while the one in the endo-cardium has not started yet. The amount of twist in the vortex is then produced every pivot turn (i.e. twice per period) and the amount of twist depends not only on the fiber rotation but also on the curvature of the tip trajectory. The higher the twist induced the larger the elongation of the vortex line and the easiest to produce breakup. The 3V-model fitted to the MBR-model produces very highly curved tip trajectories and is the reason for which breakup can occur given a specific thickness and fiber rotation rate (see Fig. 3b).

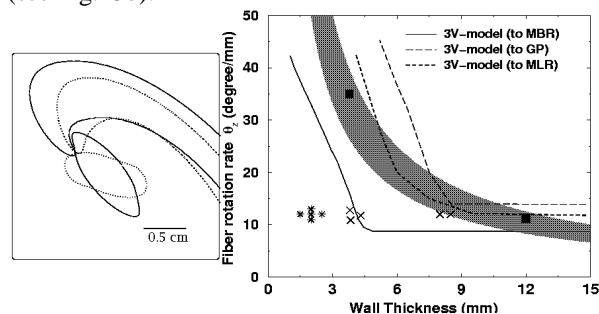


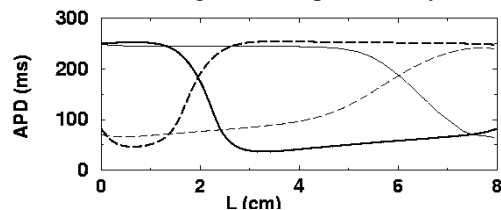
Fig. 3 (A) The rotational anisotropy is $12^\circ/\text{mm}$ in counter-clock direction from epi- to endo-cardium and the thickness of the tissue is 2.2 mm. Thick line represents the contour of the spiral and tip trajectory on the epi-cardium and the dash line on the endo-cardium. (B) Summary of simulation results using the 3V-model fitted to MBR, the LR-I model with speedup calcium, and from an experimental APD restitution (see [11]). The gray area represents mammalian hearts. The lines separates the boundaries between stable VT (bellow the

lines) and developed VF (above the lines). The MLR-model is less susceptible to VF for a given thickness because the spiral wave in the MLR-model follows a narrower pivot turn than the one in the MBR-model (see [11]).

3. Limitations of simplified ionic models.

In section 2 we showed that the simplified 3V-model reproduced very closely the APD and CV restitutions as well as the APD oscillations on a ring obtained with the original BR-model. In the two- and three-dimension simulations, the two models quantitatively have the same behavior and give very similar results, however they are not as close as one would expect from the results in section 2. The reason for this is that the simplified model does not reproduce (i) the exact shape of the AP and (ii) the precise activation and inactivation of ionic currents as function of voltage, therefore electrotonic effects are different. These effects can become important at high frequencies, for example we have shown, using the BR-model (to be published), that fast pacing can lead to spatial discordant alternans as recently shown experimentally. While the APD restitution is the cause of the discordant alternans and CV restitution helps in the induction (but is not necessary) the dynamics of the discordant regions is mostly due to electrotonic coupling (see Fig. 4). Another example where electrotonic effects can be seen is in the difference between the tip trajectories traced by the MBR-model and the 3V-model fitted to it. They have the same length and similar pivot turn, however the overall shape is somehow different as shown in [11] because of the interactions between wave fronts and backs at the high frequency of spiral rotation

Fig.4 Discordant alternans generated on a 1D string of tissue when the edge $x=0$ is periodically stimulated at



310 ms using the BR-model (darker lines) and the 3V-model (lighter lines). Solid-line shows the APD distribution at odd-beats and dash-line at even-beats. Notice that even though the restitutions are almost the same (Fig. 1) the distribution is completely different because of electrotonic effects.

4. Conclusions

Simplified models of cardiac dynamics have been proven to be valuable in the study of arrhythmias when extensive and time consuming simulations are required. It allows to vary parameters and study different levels of complexity in a shorter time. Results then can be tested

with just key simulations using the more complex models. We have shown that regions close to the apex as well as the anisotropic fiber architecture of the left ventricular wall are major predisposing factors for the degeneration of VT to VF. We also have shown that electrotonic effects can be important in some cases. Therefore future realistic simulations may need to consider the differences in AP shape found from epi- to end-cardium including the M-cells. Part of this work has been done in collaboration with A. Karma, H. Hastings and S. Evans, I thank them for their support.

References

- [1] Wiener N, Rosenblueth A. The mathematical formulation of the problem of conduction of impulses in a network of connected excitable elements, specifically in cardiac muscle. *Archos. Inst. Cardiol. Mex.* 1946; 16:205-265
- [2] Mines, G.R., On the circulating excitations in heart muscle and their possible relation to tachycardia and Fibrillation. *Trans. R. Soc.* 1914;8:43-53
- [3] Garrey W, The Nature of fibrillary contraction of the heart: its relation to tissue mass and form. *Amer. J. Physiol.* 1914: 33;397-414
- [4] Moe G, Rheinboldt W, Abildskov, A computer model of atrial fibrillation. *Am. Heart J.*;1964:67:200-220
- [5] Courtemanche M., Complex spiral wave dynamics in a spatially distributed ionic model of cardiac electrical activity. *Chaos*, 1996: 6: 579
- [6] Karma A, Electrical alternans and spiral wave breakup in cardiac tissue. *Chaos*, 1994: 4: 461-472
- [7] Hodgkin A, Huxley A, A quantitative description of membrane current and its application to conduction and excitation nerve. *J. Physiol.* 1952;117: 500-540
- [8] Beeler G, Reuter H, Reconstruction of the AP of ventricular myocardial fiber. *J. Physiol.* 1977; 268:177-219
- [9] Luo C, Rudy Y, A model of the ventricular cardiac action potential. *Circ. Res.* 1991;68:1501-1526
- [10] DiFrancesco, Noble, A model of cardiac electrical activity incorporating ionic pumps and concentration changes. *Phil. Trans. Roy. Soc. London B*, 1985;307:353-398
- [11] Fenton F, Ph.D. Thesis, Theoretical investigation of spiral and scroll wave instabilities underlying cardiac Fibrillation. Northeastern Univ. Boston, 1999.
- [12] Fenton F, Karma A, Vortex dynamics in three-dimensional continuous myocardium with fiber rotation: filament instability and fibrillation, *Chaos*;1998:8:20-47
- [13] Frame L, Simson M, Oscillations of conduction, AP duration and refractoriness *Circ.* 1988;78:1277-1287
- [14] Courtemanche, Glass, Keener, Instabilities of a propagating pulse in a ring of excitable media, *Phys. Rev. Lett.* 1993;70:2182-2185
- [15] Courtemanche, Winfree A, Re-entrant rotating waves in a BR based model of 2D cardiac electrical activity, *Int. J. Bifurcation and Chaos Appl. Sci. Eng.* 1991:1;431-444
- [16] Yermakova Y, et al. Interaction of Helical and flat periodic autowaves in an active medium. *Biophysics* 1986; 31: 348-354
- [17] Fenton F, Karma A, Fiber-rotation-induced vortex turbulence in thick myocardium. *PRL* :1998; 81:481-484